

Article

Oxygen-Resistant Electrochemiluminescence System with Polyhedral Oligomeric Silsesquioxane

Ryota Nakamura, Hayato Narikiyo, Masayuki Gon, Kazuo Tanaka *  and Yoshiki Chujo

Department of Polymer Chemistry, Graduate School of Engineering, Kyoto University, Katsura, Nishikyo-ku, Kyoto 615-8510, Japan

* Correspondence: tanaka@poly.synchem.kyoto-u.ac.jp

Received: 19 June 2019; Accepted: 7 July 2019; Published: 10 July 2019



Abstract: We report the oxygen-resistant electrochemiluminescence (ECL) system from the polyhedral oligomeric silsesquioxane (POSS)-modified tris(2,2'-bipyridyl)ruthenium(II) complex (Ru-POSS). In electrochemical measurements, including cyclic voltammetry (CV), it is shown that electric current and ECL intensity increase in the mixture system containing Ru-POSS and tripropylamine (TPrA) on the indium tin oxide (ITO) working electrode. The lower onset potential (E_{onset}) in CV is observed with Ru-POSS compared to tris(2,2'-bipyridyl)ruthenium(II) complex ($\text{Ru}(\text{bpy})_3^{2+}$). From the series of mechanistic studies, it was shown that adsorption of Ru-POSS onto the ITO electrode enhances TPrA oxidation and subsequently the efficiency of ECL with lower voltage. Moreover, oxygen quenching of ECL was suppressed, and it is proposed that the enhancement to the production of the TPrA radical could contribute to improving oxygen resistance. Finally, the ECL-based detection for water pollutant is demonstrated without the degassing treatment. The commodity system with $\text{Ru}(\text{bpy})_3^{2+}$ is not applicable in the absence of degassing with the sample solutions due to critical signal suppression, meanwhile the present system based on Ru-POSS was feasible for estimating the amount of the target even under aerobic conditions by fitting the ECL intensity to the standard curve. One of critical disadvantages of ECL can be solved by the hybrid formation with POSS.

Keywords: electrochemiluminescence; POSS; ruthenium(II) complex; oxygen resistance

1. Introduction

Electrochemiluminescence (ECL), also called as electrogenerated chemiluminescence, is light emission from the excited species generated through multiple redox reactions on an electrode [1,2]. ECL has many advantages as a platform of sensing materials. Owing to unnecessary light excitation, background noise in the luminescence detection can be drastically reduced by removing scattering of incident light. Compared to chemiluminescence which is produced through chemical reactions, it is relatively easy to achieve temporal and spatial control for emission generation. Therefore, the ECL techniques are recognized as a powerful analytical tool and are used in various areas, such as immunoassay, genosensors, and for monitoring small molecules [1–6]. Although a variety of substances can potentially work as a source of ECL, ruthenium(II) (Ru(II)) complexes, especially tris(2,2'-bipyridyl)ruthenium(II) ($\text{Ru}(\text{bpy})_3^{2+}$), are conventionally used because of many superior properties, such as high chemical stability, recyclability, redox properties, and long lifetime in the excited state [2–4]. Meanwhile, oxygen is well known to be a crucial quencher to the photo-excited state of Ru(II) complexes [7–9], followed by the reduction of the ECL intensity [10–12]. Thereby, pretreatments for deoxygenation with the analytical samples are essential before conventional ECL detection. Hence, improvement of oxygen resistance of the ECL system is strongly needed not only for improving accuracy and sensitivity in detection but also for extending applicability to future sensing technologies such as real-time monitoring with the native samples.

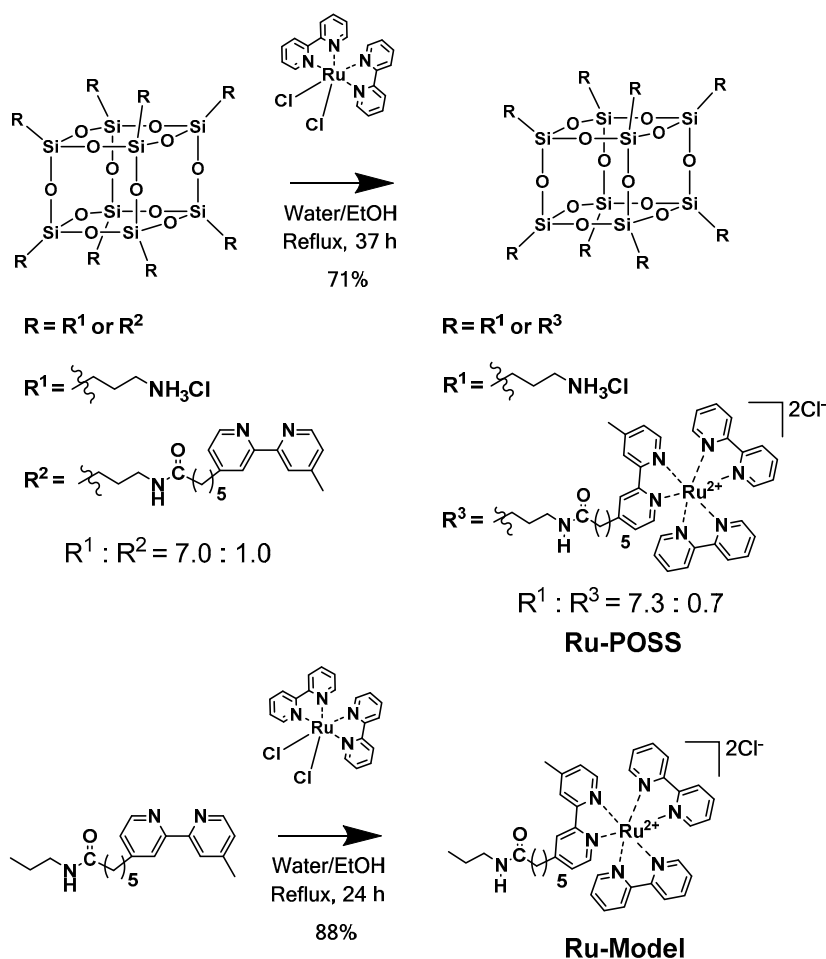
Polyhedral oligomeric silsesquioxane (POSS) attracted attention as an “element-block” which is the minimum unit containing heteroatoms for constructing functional materials [13,14]. We report unique and useful properties of POSS-containing hydrophilic materials [15–19]. In aqueous media, it was shown that the water-soluble POSS-containing materials can efficiently capture various types of guest molecules in the distinct hydrophobic spaces created around the POSS units and are applicable for sensors [20–24]. It is proposed that the cubic core is favorable for adsorbing various guest molecules with hydrophobic interaction. In particular, it is shown that the captured molecules in the POSS-core dendrimer are protected from photobleaching. It should be noted that stimuli responsiveness is compatibly observed from the captured guest molecules, although these molecules are isolated by POSS. Because of the steric structure of POSS, accessibility of reactive oxygen species which are promised to induce degradation can be lowered. Meanwhile, energy and electron transferring is acceptable through the POSS scaffold. Owing to these characters, environment-responsive photon upconversion including multiple energy transferring steps [23] and photo-triggered redox reactions [24] are accomplished in the POSS-containing materials.

Inspired by the enhancement of environmental resistance of POSS without losses of stimuli responsiveness, we presume that oxygen resistance in ECL systems might be reinforced. On the basis of this assumption, we synthesize the modified POSS tethered to the tris(2,2'-bipyridyl)ruthenium(II) complex (Ru-POSS) and evaluate the influence of dissolved oxygen on the ECL properties in the aqueous mixture system containing tripropylamine (TPrA, coreactant). Initially it is shown that ECL intensity and electric current can be enlarged by the connection to POSS. Moreover, from the comparison studies, it is clearly indicated that ECL quenching by oxygen is suppressed in the Ru-POSS/TPrA system. We elucidate how this phenomenon could originate from the improvement of TPrA oxidation by Ru-POSS adsorption onto the ITO electrode. Finally, we also accomplish the ECL-based detection for the water pollutant without the degassing pretreatment. The oxygen-resistance enhancement and target detection which tend to show the trade-off relationship are compatible by employing the POSS element-block.

2. Results and Discussion

2.1. Characteristics of Ru-POSS

The chemical structures and preparation of the Ru(II)-containing materials involving Ru-POSS and the model compound, Ru-Model are shown in Scheme 1. As is often the case with luminescent dyes, concentration quenching is occasionally induced through non-specific intermolecular interaction in the accumulation of the chromophores. To avoid reduction of sensitivity, we designed Ru-POSS to have the single Ru(II) complex. To obtain the target material, we used octa-substituted ammonium POSS (Amino-POSS) as a scaffold and connected it to the bipyridine ligand for complexation with the Ru(II) ion [24]. After complexation with the commodity reaction condition, the introduction ratio of the Ru(II) complex to the POSS unit in Ru-POSS was estimated from the integration ratios of the signal peaks from the side chains in the ^1H NMR spectrum. Purification with Ru-POSS was only precipitation and Ru-POSS was obtained as mixtures containing variable numbers of the Ru complex. The structures of synthesized compounds were confirmed by ^1H , ^{13}C and ^{29}Si NMR spectroscopies and high-resolution mass spectrometry (HRMS). The detailed procedures are shown in the Supporting Information. The structures of the compounds used, such as $\text{Ru}(\text{bpy})_3^{2+}$, $\text{Ru}(\text{bpy})_2(\text{dmbpy})^{2+}$ (dmbpy = dimethylbipyridine) and tripropyl amine (TPrA), are listed in Figure S1.



Scheme 1. Syntheses of the Ru-POSS and the Ru-Model.

2.2. ECL Properties of Ru(II)-Containing Materials

Optical measurements were performed to evaluate the influence on the electronic structure of the Ru complex moiety by the connection with POSS (Figure S2). ECL and photoluminescence (PL) spectra of the materials are shown in Figure 1 and Table 1. All compounds containing Ru(II) exhibited the emission bands at similar positions, indicating that ECL originated from the metal-to-ligand charge transfer transition in the triplet excited state (³MLCT) in the Ru(II) complex moiety [2–4]. By subtracting TPrA or Ru(bpy)₃²⁺, critical reduction of electric currents was obtained (Figure S3), supporting the conclusion that ECL is produced from the redox cycles including the Ru(II) complex and TPrA through the several proposed mechanisms (Scheme S1). The increase in the Ru(bpy)₃²⁺ concentration was minimally influenced on the enhancement of ECL intensity (Figure S4). Concentration quenching could occur under condensed conditions. Slight bathochromic shifts were observed in UV–vis absorption and ECL spectra of the solutions containing Ru-POSS and Ru-Model compared to the ECL spectrum of Ru(bpy)₃²⁺. It is likely that a substituent effect is responsible for these negligible changes [25]. From these results it was shown that electronic structure at the Ru(II) complex moiety is hardly influenced by connecting to the POSS unit.

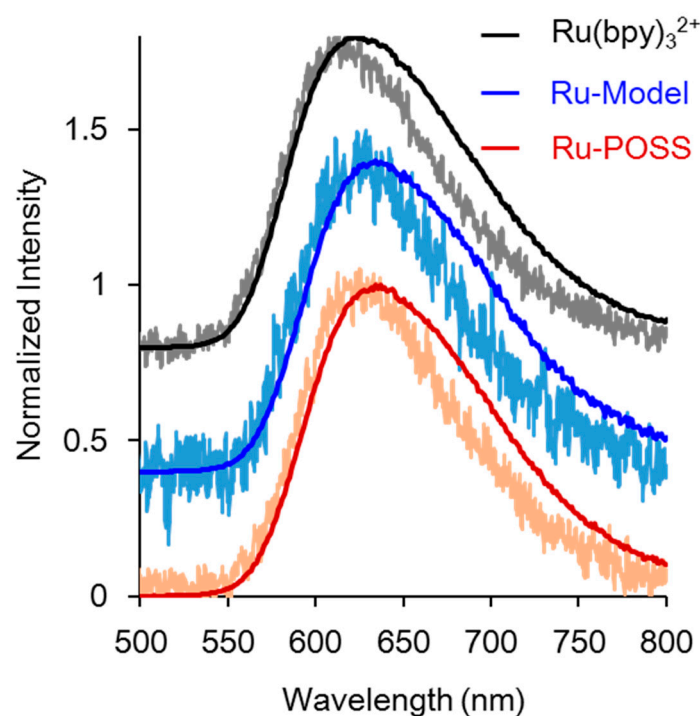


Figure 1. ECL (jagged line) and PL spectra (smooth line) of the Ru(II)-containing materials. The spectra of $\text{Ru}(\text{bpy})_3^{2+}$ and Ru-Model are shifted in the y -axis direction for clarity.

Table 1. Luminescent properties of the Ru(II)-containing materials ^a.

Compounds	$\lambda_{\text{abs_LC}}$ (nm)	$\lambda_{\text{abs_MLCT}}$ (nm)	$\lambda_{\text{em_PL}}$ (nm) ^b	Φ_{PL} (%) ^c	τ (μs) ^d	$\lambda_{\text{em_ECL}}$ (nm)	Intensity ($\times 10^4$ a.u.) ^e
Ru-POSS	286	456	634	5.6	0.44	607	13.5
Ru-Model	286	456	632	5.8	0.43	631	9.5
$\text{Ru}(\text{bpy})_3^{2+}$	286	454	623	6.3	0.50	632	8.8

^a Based on the concentration of the Ru(II) complex unit (1.0×10^{-5} M). ^b Excited at $\lambda_{\text{abs_MLCT}}$. ^c Calculated as an absolute value. ^d Measured with the excitation light at 375 nm. ^e Determined at the peak value in CV experiments.

The cyclic voltammograms and corresponding ECL profiles in the TPrA co-reactant system are shown in Figure 2. The POSS unit in Ru-POSS induced significant changes in electric and optical properties. There are two advantageous issues resulting from the connection of the Ru(II) complex to POSS. First, it was found via Ru-POSS that ECL appeared in the lower voltage region. HOMO energy levels were estimated from the onset values (E_{onset}) in the oxidative wave of the CV curves (Figure S5). Obviously, the E_{onset} of Ru-POSS decreased compared to the Ru-Model, as well as $\text{Ru}(\text{bpy})_3^{2+}$. Although it was reported that the substituent effect can decrease E_{onset} [26], the degree of change was several times larger by the connection to POSS than those in the previous work. In our ECL system, another pathway for decreasing E_{onset} could exist. Additionally, even in the absence of TPrA, lower E_{onset} values were obtained from the Ru(II)-containing materials except for $\text{Ru}(\text{bpy})_3^{2+}$ (Figure S6), proposing that the lowering value of E_{onset} might be induced by changes in molecular morphology on the electrode. The discussion will be made in a later section. Second, a larger anodic current and ECL intensity were obtained from Ru-POSS than those from $\text{Ru}(\text{bpy})_3^{2+}$ and Ru-Model. To understand the roles of POSS in these changes, further experiments were executed.

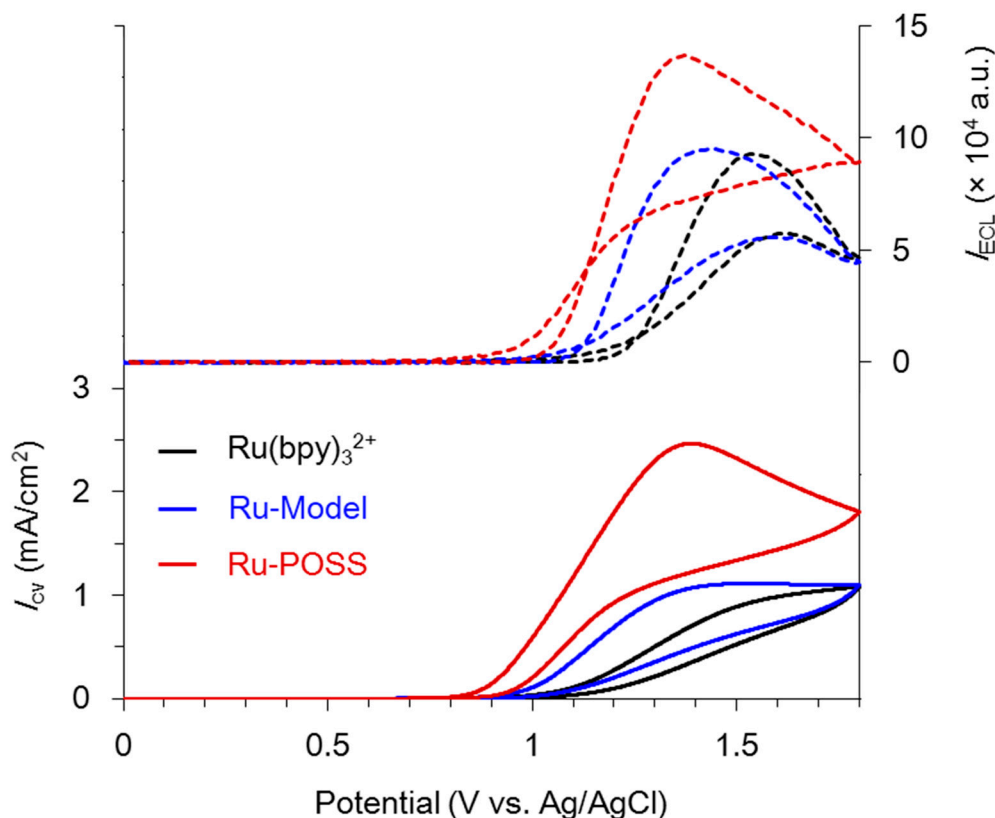


Figure 2. Cyclic voltammograms (solid lines) and corresponding ECL profiles (dashed lines) of 0.1 mM Ru(II) complexes and 100 mM TPrA in 0.20 M PBS buffer (pH 8.8) with an ITO electrode at a scan rate of 100 mV/s ($n = 3$). The concentration of Ru-POSS was based on the Ru(II) complex unit.

In the bulk electrolysis (BE) at 1.2 V vs. Ag/AgCl, it was also observed that a larger current was able to be generated from Ru-POSS than those of Ru(bpy)₃²⁺ and Ru-Model (Figure S7). In particular, the initial non-faradaic current was one order magnitude larger. To explain these behaviors, including lower E_{onset} , we initially investigated the possibility that Ru-POSS could adsorb at the electrode surfaces and accelerate the redox reactions. To evaluate the validity of this speculation, we examined BE with Ru(bpy)₃²⁺ in the presence of Amino-POSS under the same condition as above (Figure S8). It was clearly indicated that the connection to POSS was essential for obtaining a larger ECL. Next, the electrodes modified by immobilization of Ru(II) complexes were prepared, and their properties were examined. The ITO electrode was immersed in the ECL reaction solution containing the series of Ru(II) complexes, such as Ru-POSS, Ru(bpy)₃²⁺ and Ru-Model, rinsed with deionized water and dried in vacuo. Then, the BE and ECL properties were evaluated in the buffer solution containing only TPrA without adding Ru(II)-containing molecular species in the solution (Figures S9–S11). The reduction in current intensity and disappearance of ECL were observed in the ITO electrodes treated with Ru(bpy)₃²⁺ and Ru-Model, while a large current and ECL were still detected in the Ru-POSS-immersed ITO electrode. This data clearly indicated that the adsorption of Ru-POSS occurred on the ITO electrode. It has been reported that ammonium groups can form tight interaction to the ITO electrode from the studies regarding self-assembling monolayers [27–29], poly-L-lysine [30–32], and cytochrome C [33]. It is likely that the multiple ammonium groups in Ru-POSS play a critical role in adsorption to the electrode. Moreover, from the adsorption experiments under variable pH conditions, enhancement of ECL was observed by using the modified ITO electrode immersed with Ru-POSS solution in an acidic condition (pH 5.2), supporting the conclusion that the ammonium-ITO interaction is responsible for anchoring Ru-POSS onto the electrode surface (Figure S12). The assembly of functional groups into the compact space as well as the high symmetry of POSS might be favorable for tight interaction.

Regarding the lowering E_{onset} , it was reported that modification of ITO electrodes with CNT [34], poly(amidoamine) (PAMAM) dendrimer [35], Au nanoparticles [36], and thin film consisting of vertically aligned silica mesochannels [37] lowered the onset potentials and enhanced ECL intensities by facilitating the redox cycles at the electrode surfaces. Similar to these modifications, it is proposed that Ru-POSS could promote the redox cycles for the generation of ECL. Bard et al. reported about the influence of molecular morphology on intensity. They claimed that some degree of distance would be needed for obtaining emission from the Ru(II) complex adsorbed to electrodes, otherwise direct quench by the electrode would occur [38]. From our experiments, although POSS could induce adsorption of Ru(II) species on the electrode, larger ECL was obtained. It is implied that steric hindrance of the silica cube might prevent quenching by the electrode.

2.3. Resistance to Oxygen Quenching

Oxygen resistance of this ECL system was evaluated (Figure 3 and Table 2). To examine the influence of oxygen on the luminescent and electric properties, the dissolved oxygen (DO) levels in the samples were tuned by argon (DO: less than 1 mg/mL) and oxygen bubbling (ca. 20 mg/mL) before monitoring. As readily expected, the aerated sample containing Ru-complex showed critical annihilation of ECL prepared by oxygen bubbling, whereas significant influence were hardly observed in the electric currents (Figure S13). It is well known that DO readily facilitates non-radiation decay of the triplet-excited state, resulting in emission annihilation. In contrast, it was shown that the intensity level from the hypoxic sample containing Ru-POSS was maintained at the higher DO level. These data clearly indicated that the connection of Ru-complex to POSS was responsible for improving oxygen resistance in the ECL system.

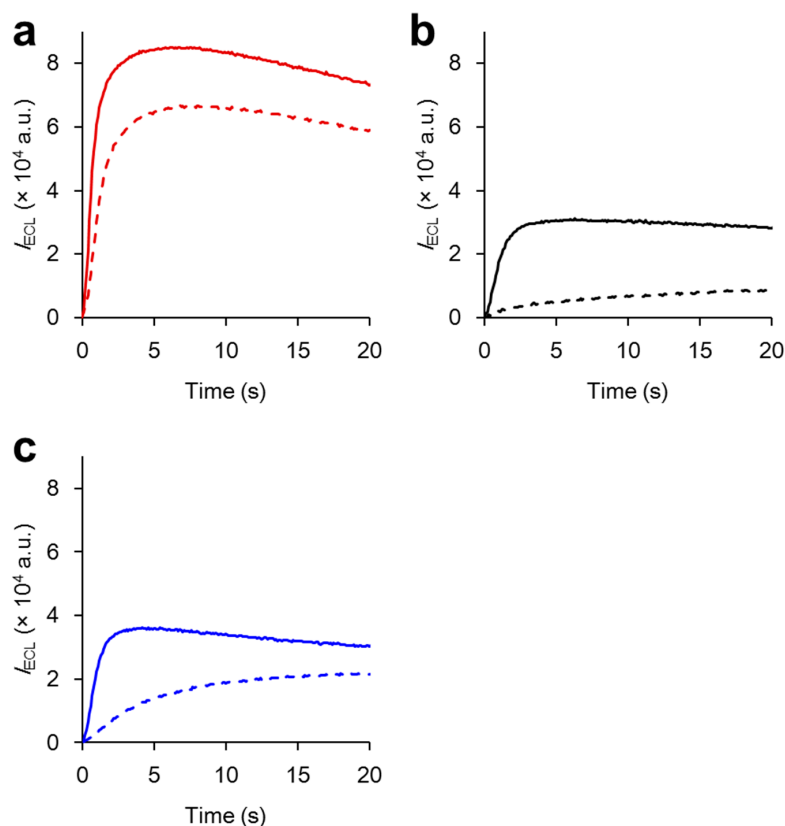


Figure 3. Time courses of ECL with (a) Ru-POSS, (b) $\text{Ru}(\text{bpy})_3^{2+}$ and (c) Ru-Model in BE with 0.1 mM Ru(II) complexes and 100 mM TPrA in 0.20 M PBS buffer (pH 8.8) with Ar (solid line) and O_2 bubbling (dashed line) with an ITO electrode at 1.2 V vs. Ag/AgCl. The concentration of Ru-POSS was based on a Ru(II) complex unit.

Table 2. Residual rates of maximum ECL intensities and onset increase rates in BE in the aerated solutions compared to the hypoxic ones.

Compounds	$I_{\text{ECL}}^{\text{Max_O}_2}/I_{\text{ECL}}^{\text{Max_Ar}}$ (%)	$m_{\text{ECL}}^{\text{Max_O}_2}/m_{\text{ECL}}^{\text{Max_Ar}}$ (%)
Ru-POSS	78	51
Ru(bpy) ₃ ²⁺	38	9
Ru-Model	61	13

m: Slope of onset intensity curve.

To obtain further insight regarding the detailed mechanism and the role of POSS in enhanced oxygen resistance, we performed measurements under various conditions. It was shown that the connection of the Ru(II) complex was necessary for expressing oxygen resistance in the former section (Figure S8 and Table S1). From the PL measurement with the Ru-POSS sample under the aerated condition, it was found that emission annihilation was induced (Figure S14), meaning that oxygen access for the Ru(II) complex moiety could be maintained even in the presence of POSS. Therefore, it was proposed that the rate of TPrA oxidation could be significantly enhanced in the Ru-POSS system. The pH effect on ECL of Ru-POSS was initially investigated (Figure S15 and Table S2). The ECL intensities of all Ru(II)-containing materials drastically decreased under acidic conditions. It should be emphasized that even in the Ru-POSS system, which had high resistance against DO, a lower intensity was shown at pH 5.2 than that at pH 8.8. According to previous literature, deprotonation in TPrA followed by oxidation of TPrA [39–41] could be suppressed under acidic conditions. Therefore, the redox cycle for generating ECL should be inhibited. It is already known that there are several pathways in the ECL mechanism of Ru(bpy)₃²⁺/TPrA system (Scheme S1) [12,40–44]. In these mechanisms, the TPrA oxidation should be the critical step before presenting luminescence. Furthermore, it was reported that the excess amount of TPrA radicals (TPrA•) generated by the TPrA oxidation can contribute to reducing of the amount of DO near the ECL reaction layer and subsequently can suppress ECL quenching [12]. In summary, the enhancement of the TPrA oxidation by Ru-POSS might be responsible for improving oxygen resistance in the ECL system as well as ECL intensity.

2.4. Analysis of Antibiotics without Deoxygenation

Because ECL is usually obtained from the triplet-excited state, most conventional ECL systems always suffer from emission quenching by DO in the pristine sample. Therefore, degassing for lowering DO levels in the sample was previously needed in practical usage. To demonstrate the advantage of oxygen-resistant ECL based on Ru-POSS, we finally performed the detection without degassing as a pre-treatment. By evaluating the decrease in ECL intensity, the target concentration was determined [45–49]. By adding oxytetracycline (OTC), which is an anti-bacterial agent for domestic animals that often induces water pollution near livestock barns, to the samples, the changes in ECL intensity were monitored. The OTC aqueous solution was added to the buffer containing 0.1 mM Ru(II) complex and 0.1 M TPrA with stirring and then ECL measurements in BE (1.2 V vs. Ag/AgCl) of the mixtures were taken (Figure 4). Apparently, ECL intensity from the Ru(bpy)₃²⁺/TPrA system was too small to discriminate the target, meanwhile critical decrease in emission intensity was detected from the Ru-POSS sample, meaning that the existence of OTC was able to be detected even in the aerobic sample. In particular, the linear relationship between ΔI_{ECL} and the concentration in the range from 1.3×10^{-5} to 2.0×10^{-4} M ($R^2 = 0.993$) was obtained when using Ru-POSS. The limit of detection was 9.8×10^{-6} M (S/N = 3). It was suggested that ECL quenching may be caused by oxidized OTC at the electrode, which is a benzoquinone derivative [45]. Benzoquinone groups are well known to have the ability to quench ECL [48,49]. The decay of the excited state of the Ru(II) complex and TPrA intermediate-radical quenching were induced by benzoquinone and the latter pathway was predominant when TPrA direct oxidation occurred [49]. Regarding the detection limit, it has been reported that the OTC concentrations in wastewater are in the range between 10^{-6} and 10^{-9} M

order [47]. The detection limit of our system was not so high compared with the other ECL system [45], however, our method could be directly applicable for detecting serious contaminated conditions.

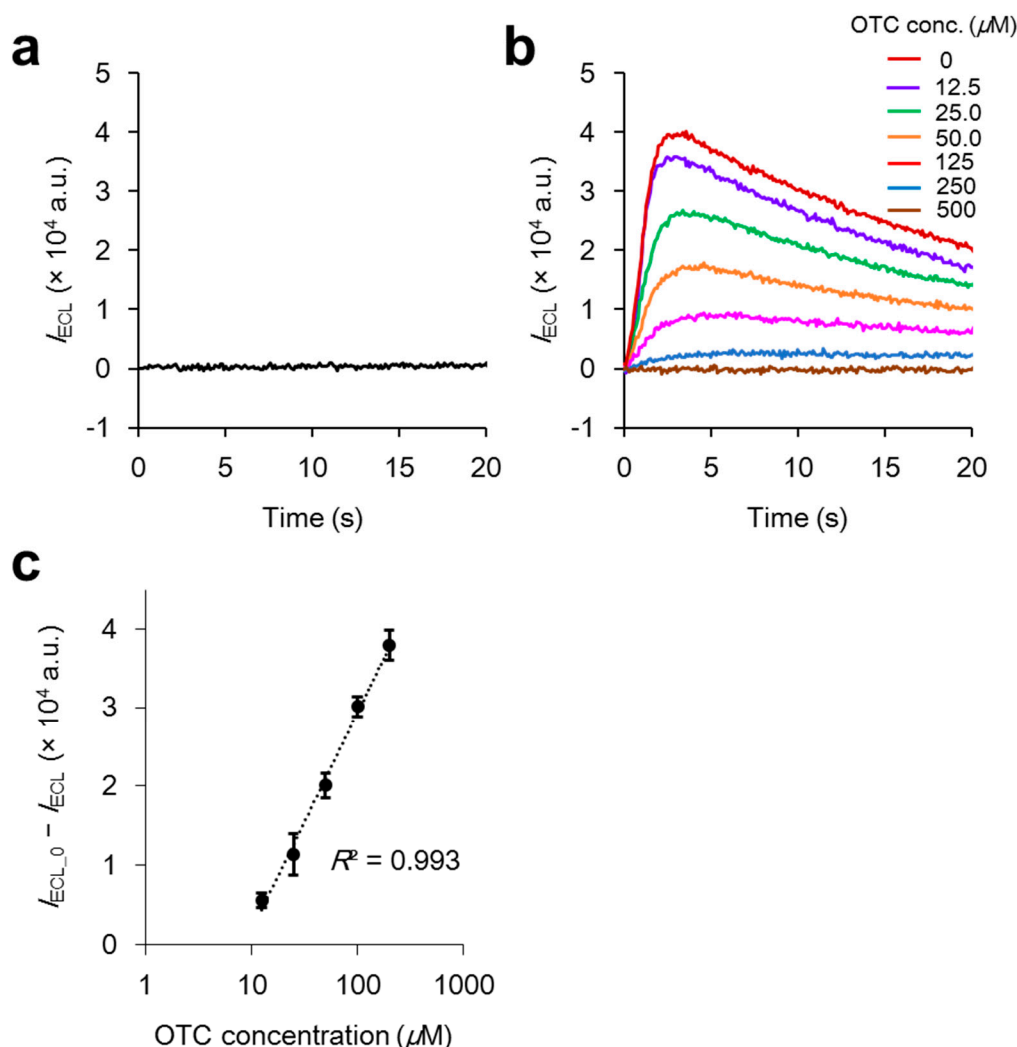


Figure 4. Time courses of ECL with (a) Ru(bpy)₃²⁺ and (b) Ru-POSS in BE of 0.1 mM Ru(II) complexes and 100 mM TPrA and various concentrations of OTC in 0.20 M PBS buffer (pH 8.8) stirred for 20 min with an ITO electrode at 1.2 V vs. Ag/AgCl. (c) Standard curve prepared from the data from (b) (I_{ECL} and I_{ECL_0} represent the maximum ECL intensity in the time course of BE with and without OTC, respectively).

3. Conclusions

We demonstrate the Ru(II) complex-modified POSS and its application for oxygen-resistant ECL system. By employing POSS, various beneficial effects were obtained. Electronic currents and ECL intensities were enhanced in the electro- and optical measurements, and E_{onset} in CV was lowered compared to Ru(bpy)₃²⁺. Moreover, ECL quenching by oxygen was suppressed in the Ru-POSS/TPrA system. From our mechanistic studies, adsorption of Ru-POSS to the ITO electrode, followed by efficient TPrA oxidation on the ITO electrode were suggested. Finally, oxygen quenching was compensated by generation of the TPrA radical. Our findings and materials could be a scaffold for developing future sensing technologies based on ECL, such as real-time monitoring for small molecular pollutants which it is difficult to detect with conventional environment sensors. Furthermore, compared to the conventional system, the oxygen-resistance can be improved by connecting to POSS at this stage. As mentioned in the introduction, POSS has significant properties for capturing hydrophobic molecules

under aerobic conditions. In combination with the unique capturing property of the POSS unit, improvement of sensitivity and selectivity for the target detection might be proposed.

Supplementary Materials: The following are available online at <http://www.mdpi.com/2073-4360/11/7/1170/s1>, Figure S1: Structures of $\text{Ru}(\text{bpy})_3^{2+}$, $\text{Ru}(\text{bpy})_2(\text{dmbpy})^{2+}$ and TPrA, Figure S2: (a) UV–vis absorption and (b) PL spectra of 1.0×10^{-5} M solutions containing $\text{Ru}(\text{bpy})_3^{2+}$, Ru-Model and Ru-POSS in H_2O . The excitation light at $\lambda_{\text{abs_MLCT}}$ was used for PL measurements. Inset figure in (a) is the inset around the MLCT band. The concentration of Ru-POSS was based on the Ru(II) complex unit, Figure S3: Cyclic voltammograms of 0.10 mM $\text{Ru}(\text{bpy})_3^{2+}$ and/or 0.1 M TPrA in 0.20 M PBS buffer (pH 8.8) at ITO electrode at a scan rate of 100 mV/s ($n = 3$), Figure S4: Time courses of ECL in BE of 0.50 mM $\text{Ru}(\text{bpy})_3^{2+}$ and 100 mM TPrA in 0.20 M PBS buffer (pH 8.8) with deoxygenation (solid line) or aeration (dashed line) with an ITO electrode at 1.2 V vs. Ag/AgCl, Figure S5: The determination of onset potential (E_{onset}). The onset potentials were determined from the intersection of the tangents between the baseline and the signal current, Figure S6: Cyclic voltammograms of 0.10 mM Ru(II)-containing materials in 0.20 M PBS buffer (pH 8.8) with an ITO electrode at a scan rate of 100 mV/s ($n = 3$). The concentration of Ru-POSS was based on the Ru(II) complex unit, Figure S7: Initial time courses of current in BE of 0.10 mM Ru(II) complexes and 100 mM TPrA in 0.20 M PBS buffer (pH 8.8) at ITO electrode at 1.2 V vs. Ag/AgCl ($n = 3$). The concentration of Ru-POSS was based on the Ru(II) complex unit, Figure S8: Time courses of ECL with 0.1 mM $\text{Ru}(\text{bpy})_3^{2+}$, 0.1 mM Amino-POSS and 100 mM TPrA in 0.20 M PBS buffer (pH 8.8) with Ar (solid line) and O_2 bubbling (dashed line) with an ITO electrode at 1.2 V vs. Ag/AgCl, Figure S9: Time courses of ECL in BE of 100 mM TPrA in 0.20 M PBS buffer (pH 8.8) with the modified ITO electrodes at 1.2 V vs. Ag/AgCl, Figure S10: Cyclic voltammograms (solid lines) and corresponding ECL curves (dashed lines) at a scan rate of 100 mV/s with 0.1 mM Ru-POSS and 100 mM TPrA in 0.20 M PBS buffer (pH 8.8) with an ITO electrode (Red line) and 100 mM TPrA in 0.20 M PBS buffer (pH 8.8) with the modified ITO electrode (Blue line). The concentration of Ru-POSS was based on the Ru(II) complex unit, Figure S11: Time courses of currents with (a) Ru-POSS (b) $\text{Ru}(\text{bpy})_3^{2+}$ (c) Ru-Model in BE of 100 mM TPrA in 0.20 M PBS buffer (pH 8.8) with (solid line) or without 0.10 mM Ru(II) complexes (dashed line) at ITO electrode at 1.2 V vs. Ag/AgCl ($n = 3$). The concentration of Ru-POSS was based on the Ru(II) complex unit, Figure S12: Time courses of ECL in BE of 100 mM TPrA in 0.20 M PBS buffer (pH 8.8) at 1.2 V vs. Ag/AgCl with the modified ITO electrodes immersed into the solution containing 0.1 mM Ru-POSS (based on the Ru(II) complex unit) with 100 mM TPrA in 0.20 M PBS buffer with variable pH values (pH 5.2: orange line and pH 8.8: blue line), Figure S13: Time courses of electric currents with (a) Ru-POSS, (b) $\text{Ru}(\text{bpy})_3^{2+}$, (c) Ru-Model and (d) $\text{Ru}(\text{bpy})_3^{2+}$ + Amino-POSS in BE of 0.10 mM Ru(II) complexes and 100 mM TPrA in 0.20 M PBS buffer (pH 8.8) with Ar (solid line) and O_2 bubbling (dashed line) with and ITO electrode at 1.2 V vs. Ag/AgCl. The concentration of Ru-POSS was based on a Ru(II) complex unit. The concentration of Amino-POSS in (d) was adjusted to the same as the POSS unit in (a), Figure S14: Residual rates of emission intensities of the photo-excited Ru(II) complexes in aerated solutions consist of 0.01 mM Ru(II) complexes and 0.1 M TPrA in 0.2 M PBS solution (pH 8.8). Excitation wavelengths were $\lambda_{\text{abs_MLCT}}$ Residual rates were calculated from the equation, $I_{\text{PL_Air}}/I_{\text{PL_Ar}}$, where $I_{\text{PL_Air}}$ is the intensity at $\lambda_{\text{em}}^{\text{max}}$ in aerated solutions and $I_{\text{PL_Ar}}$ is in the hypoxic solutions, Figure S15: Cyclic voltammograms (solid lines) and corresponding ECL curves (dotted lines) of 0.1 mM Ru(II) complexes and 100 mM TPrA in 0.20 M PBS buffer (pH 5.2) with an ITO electrode at a scan rate of 100 mV/s ($n = 3$). The concentration of Ru-POSS was based on a Ru(II) complex unit, Table S1: Residual rates of maximum ECL intensities and onset increase rates in BE in the aerated solution compared to the hypoxic one, Table S2: E_{onset} in various conditions. Scheme S1: The summary of the ECL mechanisms in the $\text{Ru}(\text{bpy})_3^{2+}$ /TPrA system ($\text{TPrA}^{\bullet+} = \text{Pr}_3\text{N}^{\bullet+}$, $\text{TPrA}^{\bullet} = \text{Pr}_2\text{NC}^{\bullet}\text{HCH}_2\text{CH}_3$, $\text{P}_1 = \text{Pr}_2\text{N}^+\text{CHCH}_2\text{CH}_3$).

Author Contributions: Conceptualization, K.T.; data curation, R.N., H.N. and M.G.; funding acquisition, K.T. and Y.C.; investigation, R.N. and H.N.; project administration, K.T.; supervision, K.T.; writing—original draft, R.N., M.G. and K.T.; writing—review and editing, Y.C.

Funding: This work was partially supported by the Kurita Water and Environment Foundation (for K.T.), a Grant-in-Aid for Scientific Research (B) (JP17H03067) and (A) (JP 17H01220) and for Scientific Research on Innovative Areas “New Polymeric Materials Based on Element-Blocks (No.2401)” (JP24102013).

Conflicts of Interest: The authors declare no conflicts of interest.

References

1. Richter, M.M. Electrochemiluminescence (ECL). *Chem. Rev.* **2008**, *104*, 3003–3036. [[CrossRef](#)]
2. Miao, W. Electrogenenerated Chemiluminescence and Its Biorelated Applications. *Chem. Rev.* **2008**, *108*, 2506–2553. [[CrossRef](#)]
3. Fähnrich, K.A.; Pravda, M.; Guilbault, G.G. Recent applications of electrogenerated chemiluminescence in chemical analysis. *Talanta* **2001**, *54*, 531–559. [[CrossRef](#)]
4. Gorman, B.A.; Francis, P.S.; Barnett, N.W. Tris(2,2'-bipyridyl)ruthenium(II) chemiluminescence. *Analyst* **2006**, *131*, 616–639. [[CrossRef](#)]

5. Qi, H.; Peng, Y.; Gao, Q.; Zhang, C. Applications of nanomaterials in electrogenerated chemiluminescence biosensors. *Sensors* **2009**, *9*, 674–695. [[CrossRef](#)]
6. Li, L.; Chen, Y.; Zhu, J.J. Recent Advances in Electrochemiluminescence Analysis. *Anal. Chem.* **2017**, *89*, 358–371. [[CrossRef](#)]
7. Demas, J.N.; Diemente, D.; Harris, E.W. Oxygen quenching of charge-transfer excited states of ruthenium(II) complexes. Evidence for singlet oxygen production. *J. Am. Chem. Soc.* **1973**, *95*, 6864–6865. [[CrossRef](#)]
8. Lin, C.T.; Sutin, N. An investigation of the micellar phase of sodium dodecyl sulfate in aqueous sodium chloride solutions using quasielastic light scattering spectroscopy. *J. Phys. Chem.* **1976**, *80*, 97–105. [[CrossRef](#)]
9. O’Keeffe, G.; McDonagh, C.M.; O’Kelly, B.; Vos, J.G.; Keyes, E.T.; McGilp, J.F.; MacCraith, B.D. fibre optic oxygen sensor based on fluorescence quenching of evanescent-wave excited ruthenium complexes in sol-gel derived porous coatings. *Analyst* **1993**, *118*, 385–388.
10. Fiaccabrino, G.C.; Koudelka-Hep, M.; Hsueh, Y.T.; Collins, S.D.; Smith, R.L. Electrochemiluminescence of Tris(2,2’-bipyridine)ruthenium in Water at Carbon Microelectrodes. *Anal. Chem.* **1998**, *70*, 4157–4161. [[CrossRef](#)]
11. Tomita, I.N.; Bulhões, L.O.S. Electrogenerated chemiluminescence determination of cefadroxil antibiotic. *Anal. Chim. Acta* **2001**, *442*, 201–206. [[CrossRef](#)]
12. Zheng, H.; Zu, Y. Emission of Tris(2,2’-bipyridine)ruthenium(II) by Coreactant Electrogenerated Chemiluminescence: From O₂-Insensitive to Highly O₂-Sensitive. *J. Phys. Chem. B* **2005**, *109*, 12049–12053. [[CrossRef](#)]
13. Kuo, S.W.; Chang, F.C. POSS related polymer nanocomposites. *Prog. Polym. Sci.* **2011**, *36*, 1649–1696. [[CrossRef](#)]
14. Chujo, Y.; Tanaka, K. New Polymeric Materials Based on Element-Blocks. *Bull. Chem. Soc. Jpn.* **2015**, *88*, 633–643. [[CrossRef](#)]
15. Gon, M.; Tanaka, K.; Chujo, Y. Recent Progress in the Development of Advanced Element-Block Materials. *Polym. J.* **2018**, *50*, 109–126. [[CrossRef](#)]
16. Gon, M.; Kato, K.; Tanaka, K.; Chujo, Y. Elastic and mechanofluorochromic hybrid films with POSS-capped polyurethane and polyfluorene. *Mater. Chem. Front.* **2019**, *3*, 1174–1180. [[CrossRef](#)]
17. Gon, M.; Sato, K.; Kato, K.; Tanaka, K.; Chujo, Y. Preparation of Bright-Emissive Hybrid Materials Based on Light-Harvesting POSS Having Radially Integrated Luminophores and Commodity π -Conjugated Polymers. *Mater. Chem. Front.* **2019**, *3*, 314–320. [[CrossRef](#)]
18. Ueda, K.; Tanaka, K.; Chujo, Y. Optical, Electrical and Thermal Properties of Organic–Inorganic Hybrids with Conjugated Polymers Based on POSS Having Heterogeneous Substituents. *Polymers* **2019**, *11*, 44. [[CrossRef](#)]
19. Ueda, K.; Tanaka, K.; Chujo, Y. Fluoroalkyl POSS with Dual Functional Groups as a Molecular Filler for Lowering Refractive Indices and Improving Thermomechanical Properties of PMMA. *Polymers* **2018**, *10*, 1332. [[CrossRef](#)]
20. Narikiyo, H.; Gon, M.; Tanaka, K.; Chujo, Y. Control of Intramolecular Excimer Emission in Luminophore-Integrated Ionic POSSs Possessing Flexible Side-Chains. *Mater. Chem. Front.* **2018**, *2*, 1449–1455. [[CrossRef](#)]
21. Narikiyo, H.; Kakuta, T.; Matsuyama, H.; Gon, M.; Tanaka, K.; Chujo, Y. Development of the Optical Sensor for Discriminating Isomers of Fatty Acids Based on Emissive Network Polymers Composed of Polyhedral Oligomeric Silsesquioxane. *Bioorg. Med. Chem.* **2017**, *25*, 3431–3436. [[CrossRef](#)]
22. Kakuta, T.; Jeon, J.-H.; Tanaka, K.; Chujo, Y. Development of Highly-Sensitive Detection System in ¹⁹F NMR for Bioactive Compounds Based on the Assembly of Paramagnetic Complexes with Fluorinated Cubic Silsesquioxanes. *Bioorg. Med. Chem.* **2017**, *25*, 1389–1393. [[CrossRef](#)]
23. Tanaka, K.; Okada, H.; Ohashi, W.; Jeon, J.-H.; Inafuku, K.; Chujo, Y. Hypoxic Conditions-Selective Upconversion via Triplet-Triplet Annihilation Based on POSS-Core Dendrimer Complexes. *Bioorg. Med. Chem.* **2013**, *21*, 2678–2681. [[CrossRef](#)]
24. Jeon, J.-H.; Tanaka, K.; Chujo, Y. Light-Driven Artificial Enzymes for Selective Oxidation of Guanosine Triphosphate Using Water-Soluble POSS Network Polymers. *Org. Biomol. Chem.* **2014**, *12*, 6500–6506. [[CrossRef](#)]
25. McClanahan, S.F.; Dallinger, R.F.; Holler, F.J.; Kincaid, J.R. Mixed-ligand poly(pyridine) complexes of ruthenium(II). Resonance Raman spectroscopic evidence for selective population of ligand-localized ³MLCT excited states. *J. Am. Chem. Soc.* **1985**, *107*, 4853–4860. [[CrossRef](#)]

26. Juris, A.; Balzani, V.; Belser, P.; VON Zelewsky, V.A. Characterization of the Excited State Properties of Some New Photosensitizers of the Ruthenium (Polypyridine) Family. *Helv. Chim. Acta* **1981**, *64*, 2175–2182. [[CrossRef](#)]
27. Oh, S.Y.; Yun, Y.J.; Kim, D.Y.; Han, S.H. Formation of a Self-Assembled Monolayer of Diaminododecane and a Heteropolyacid Monolayer on the ITO Surface. *Langmuir* **1999**, *15*, 4690–4692. [[CrossRef](#)]
28. Kim, K.; Song, H.; Park, J.T.; Kwak, J. C₆₀ Self-Assembled Monolayer Using Diamine as a Prelayer. *Chem. Lett.* **2000**, *29*, 958–959. [[CrossRef](#)]
29. Bermudez, V.M.; Berry, A.D.; Kim, H.; Piqué, A. Functionalization of Indium Tin Oxide. *Langmuir* **2006**, *22*, 11113–11125. [[CrossRef](#)]
30. Bearinger, J.P.; Vörös, J.; Hubbell, J.A.; Textor, M. Electrochemical optical waveguide lightmode spectroscopy (EC-OWLS): A pilot study using evanescent-field optical sensing under voltage control to monitor polycationic polymer adsorption onto indium tin oxide (ITO)-coated waveguide chips. *Biotechnol. Bioeng.* **2003**, *82*, 465–473. [[CrossRef](#)]
31. Yang, H.J.; Sugiura, Y.; Ishizaki, I.; Sanada, N.; Ikegami, K.; Zaima, N.; Shrivastava, K.; Setou, M. Imaging of lipids in cultured mammalian neurons by matrix assisted laser/desorption ionization and secondary ion mass spectrometry. *Surf. Interface Anal.* **2010**, *42*, 1606–1611. [[CrossRef](#)]
32. Choi, Y.; Yagati, A.K.; Cho, S. Electrochemical Characterization of Poly-L-Lysine Coating on Indium Tin Oxide Electrode for Enhancing Cell Adhesion. *J. Nanosci. Nanotechnol.* **2015**, *15*, 7881–7885. [[CrossRef](#)]
33. Koller, K.B.; Hawkrige, F.M. Temperature and electrolyte effects on the electron-transfer reactions of cytochrome c. *J. Am. Chem. Soc.* **1985**, *107*, 7412–7417. [[CrossRef](#)]
34. Valenti, G.; Zangheri, M.; Sansaloni, S.E.; Mirasoli, M.; Penicaud, A.; Roda, A.; Paolucci, F. Transparent Carbon Nanotube Network for Efficient Electrochemiluminescence Devices. *Chem. Eur. J.* **2015**, *21*, 12640–12645. [[CrossRef](#)]
35. Kim, Y.; Kim, J. Modification of Indium Tin Oxide with Dendrimer-Encapsulated Nanoparticles To Provide Enhanced Stable Electrochemiluminescence of Ru(bpy)₃²⁺/Tripropylamine While Preserving Optical Transparency of Indium Tin Oxide for Sensitive Electrochemiluminescence-Based Analyses. *Anal. Chem.* **2014**, *86*, 1654–1660.
36. Pan, S.; Liu, J.; Hill, C.M. Observation of Local Redox Events at Individual Au Nanoparticles Using Electrogenerated Chemiluminescence Microscopy. *J. Phys. Chem. C* **2015**, *119*, 27095–27103. [[CrossRef](#)]
37. Su, B.; Xu, L.; Yang, Q.; Zhou, Z.; Guo, W. Two orders-of-magnitude enhancement in the electrochemiluminescence of Ru(bpy)₃²⁺ by vertically ordered silica mesochannels. *Anal. Chim. Acta* **2015**, *886*, 48–55.
38. Miller, C.J.; McCord, P.; Bard, A.J. Study of Langmuir monolayers of ruthenium complexes and their aggregation by electrogenerated chemiluminescence. *Langmuir* **1991**, *7*, 2781–2787. [[CrossRef](#)]
39. Leland, J.K.; Powell, M.J. Electrogenerated Chemiluminescence: An Oxidative-Reduction Type ECL Reaction Sequence Using Tripropyl Amine. *J. Electrochem. Soc.* **1990**, *137*, 3127–3131. [[CrossRef](#)]
40. Miao, W.; Choi, J.P.; Bard, A.J. Electrogenerated Chemiluminescence 69: The Tris(2,2'-bipyridine)ruthenium(II), (Ru(bpy)₃²⁺)/Tri-*n*-propylamine (TPrA) System Revisited—A New Route Involving TPrA^{•+} Cation Radicals. *J. Am. Chem. Soc.* **2002**, *124*, 14478–14485. [[CrossRef](#)]
41. Zu, Y.; Li, F. Characterization of the low-oxidation-potential electrogenerated chemiluminescence of tris(2,2'-bipyridine)ruthenium(II) with tri-*n*-propylamine as coreactant. *Anal. Chim. Acta* **2005**, *550*, 47–52. [[CrossRef](#)]
42. Wightman, R.M.; Forry, S.P.; Maus, R.; Badocco, D.; Pastore, P. Rate-Determining Step in the Electrogenerated Chemiluminescence from Tertiary Amines with Tris(2,2'-bipyridyl)ruthenium(II). *J. Phys. Chem. B* **2004**, *108*, 19119–19125. [[CrossRef](#)]
43. Kanoufi, F.; Zu, Y.; Bard, A.J. Homogeneous Oxidation of Trialkylamines by Metal Complexes and Its Impact on Electrogenerated Chemiluminescence in the Trialkylamine/Ru(bpy)₃²⁺ System. *J. Phys. Chem. B* **2001**, *105*, 210–216. [[CrossRef](#)]
44. Gross, E.M.; Pastore, P.; Wightman, R.M. High-Frequency Electrochemiluminescent Investigation of the Reaction Pathway between Tris(2,2'-bipyridyl)ruthenium(II) and Tripropylamine Using Carbon Fiber Microelectrodes. *J. Phys. Chem. B* **2001**, *105*, 8732–8738. [[CrossRef](#)]

45. Pang, Y.Q.; Cui, H.; Zheng, H.S.; Wan, G.H.; Liu, L.J.; Yu, X.F. Flow injection analysis of tetracyclines using inhibited Ru(bpy)₃²⁺/tripropylamine electrochemiluminescence system. *Luminescence* **2005**, *20*, 8–15. [[CrossRef](#)]
46. Zhu, Y.; Li, B.; Liu, J.; Chen, K. Determination of p-aminobenzenesulfonic acid based on the electrochemiluminescence quenching of tris(2,2'-bipyridine)-ruthenium (II). *Luminescence* **2013**, *28*, 363–367. [[CrossRef](#)]
47. Tagiri-Endo, M.; Suzuki, S.; Nakamura, T.; Hatakeyama, T.; Kawamukai, K. Rapid determination of five antibiotic residues in swine wastewater by online solid-phase extraction-high performance liquid chromatography-tandem mass spectrometry. *Anal. Bioanal. Chem.* **2009**, *393*, 1367–1375. [[CrossRef](#)]
48. McCall, J.; Alexander, C.; Richter, M.M. Quenching of Electrogenerated Chemiluminescence by Phenols, Hydroquinones, Catechols, and Benzoquinones. *Anal. Chem.* **1999**, *71*, 2523–2527. [[CrossRef](#)]
49. Zheng, H.; Zu, Y. Highly Efficient Quenching of Coreactant Electrogenerated Chemiluminescence by Phenolic Compounds. *J. Phys. Chem. B* **2005**, *109*, 16047–16051. [[CrossRef](#)]



© 2019 by the authors. Licensee MDPI, Basel, Switzerland. This article is an open access article distributed under the terms and conditions of the Creative Commons Attribution (CC BY) license (<http://creativecommons.org/licenses/by/4.0/>).